

# ASSESSMENT OF GOMOS RETRIEVAL ALGORITHMS AND QUALITY OF LEVEL 2 PRODUCTS

M. Guirlet<sup>(1)</sup>, G. Barrot<sup>(1)</sup>, O. Fanton d'Andon<sup>(1)</sup>, A. Mangin<sup>(1)</sup>,  
V. Sofieva<sup>(2)</sup>, E. Kyrölä<sup>(2)</sup>, J. Tamminen<sup>(2)</sup>, F. Dalaudier<sup>(3)</sup>, A. Hauchecorne<sup>(3)</sup>, J.L. Bertaux<sup>(3)</sup>,  
D. Fussen<sup>(4)</sup>, F. Vanhellemont<sup>(4)</sup>, Y. Meijer<sup>(5)</sup>, T. Fehr<sup>(6)</sup>, L. Saavedra de Miguel<sup>(7)</sup>, P. Snoeij<sup>(8)</sup>

<sup>(1)</sup> ACRI-ST, 260 route du Pin Montard, 06902 Sophia-Antipolis Cedex, France,  
marielle.guirlet@acri-st.fr,

<sup>(2)</sup> Finnish Meteorological Institute, <sup>(3)</sup> Service d'Aéronomie CNRS/IPSIL, <sup>(4)</sup> BIRA-IASB, <sup>(5)</sup> RIVM,  
<sup>(6)</sup> ESA/ESRIN, <sup>(7)</sup> SERCO, <sup>(8)</sup> ESA

## ABSTRACT

In the framework of the GOMOS Quality Working Group activities, a routine assessment of GOMOS Level 2 products is performed. Besides verifying the scientific validity of the Level 2 products, these activities also support the assessment of the retrieval algorithm, and they allow to compare the performances of the processor prototype for different configurations. We present here some results illustrating this assessment exercise. Special emphasis is given to the version of the prototype used for the 1<sup>st</sup> reprocessing and to the version used for the 2<sup>nd</sup> reprocessing. This latter version corresponds to the currently operational version of the IPF.

## 1. INTRODUCTION

The quality assessment of the products retrieved from the GOMOS measurements is a routine activity. In case of configuration changes in the retrieval algorithms, it also supports the evaluation of the impact of those changes. As part of the continuous effort made for the improvement of the quality of GOMOS products, several successive IPF versions have been developed since the first delivery of products. The changes proposed by the QWG are first implemented in the most recent version of the processor prototype (GOPR) developed and maintained by ACRI. Their impact on the Level 2 products is verified and evaluated. Once approved, the configuration changes are then implemented in the IPF baseline, and this new IPF is activated for operational processing. We focus here on the two GOPR versions 6.0ab and 6.0dh, which were used for the two reprocessing activities of GOMOS measurements. All products between July 2002 and August 2006 have been reprocessed a posteriori (second reprocessing activities performed in 2006) with GOPR 6.0dh corresponding to the IPF currently in operation (version 5.00). Measurements made in 2003 and between March and December 2004 had also been retrieved a posteriori with a previous version of GOPR, 6.0ab (IPF 4.02).

We first present the main differences in the configuration of the prototype versions expected to

impact most the vertical profiles of species. An important change relates to the flagging strategy of the retrieved density values. We assess the impact of these changes on the average of the vertical profiles of species and on their dispersion, by comparing these quantities for a testing dataset retrieved with the two processor versions. The comparison of O<sub>3</sub> vertical profiles processed with the two versions to ground-based and satellite measurements also gives indications on the impact of the changes on the comparison of GOMOS data to external measurements.

Other aspects relevant to the assessment of the version 6.0dh of the retrieval algorithm are discussed and some illustrative examples are presented. The comparison of products from measurements made in very close spatial and time coincidence (the so-called GOMOS-GOMOS coincidences), and from occultations of the same star, allows to check the robustness of the retrieval. The comparison of vertical profiles from GOMOS coincident measurements for different stars may also illustrate the impact of the star characteristics on the accuracy and on the retrieval quality of the vertical profiles of local density.

Vertical profiles of local density and aerosol extinction coefficient presented here were all retrieved from occultations measured in full dark illumination conditions, except when explicitly stated.

## 2. ASSESSMENT OF SUCCESSIVE VERSIONS OF THE PROCESSOR

### 2.1. Main configuration changes

Some of the changes implemented in the Level 2 part of the processor chain of GOPR 6.0dh are presented and compared to the configuration of GOPR 6.0ab in Table 1 (see after 7. ). Level 1b changes in this new version are described in [4].

### 2.2. Impact of the flagging strategy change

Density values computed by the retrieval algorithms are stored in the Level 2 products along with flag values provided as Product Confidence Data (PCD). The PCD value provides indications on the configuration and the performance of the

processing at several stages of the retrieval. It is recommended to use only non-flagged values of the density, i.e. PCD equal to 0 (this recommendation will be applied in all the following results). In GOPR 6.0ab, negative values of density computed by the spectral inversion or by the vertical inversion were systematically flagged, which is not the case with GOPR 6.0dh. For a set of vertical profiles processed with 6.0dh, flagged values, non-flagged positive values and non-flagged negative values of  $O_3$  local density are plotted vs geometric altitude in Figure 1. Thus, from the same set of profiles, there are more non-flagged values for 6.0dh than for 6.0ab, and they will include negative values. Filtering out all the negative non-flagged values in 6.0dh may yield an artificial positive bias in statistical averages computed from a specific dataset. Instead, it is recommended to apply complementary selection criteria based on the "standard deviation" values stored in the products.

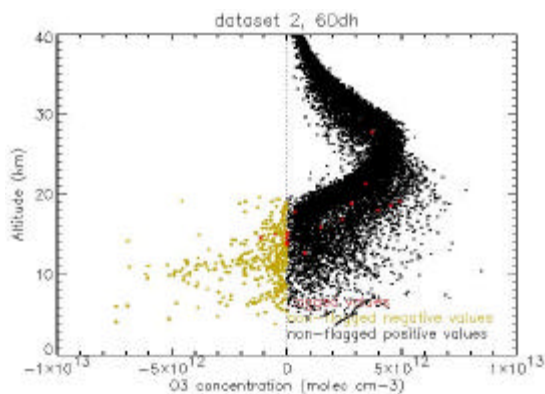


Figure 1: Values of the  $O_3$  local density vs geometric altitude for the Level 2 products of a testing dataset processed with GOPR 6.0dh. Flagged values (i.e. PCD not equal to 0) are plotted with the red dots; non-flagged negative values are plotted with the green dots; non-flagged positive values are plotted with the black dots.

### 2.3. Average and dispersion of the local density profiles

The average and the dispersion of the vertical profiles of  $O_3$ ,  $NO_2$ ,  $NO_3$  local density and aerosol extinction coefficient are compared for the same set of profiles processed with the two GOPR versions (Figure 15). We consider here a testing dataset of more than 500 occultations of star 29 measured at low latitudes between December 2002 and February 2003. At the  $O_3$  maximum level, the median value of  $O_3$  local density is about 5% higher for 6.0dh profiles than for 6.0ab profiles. The dispersion (calculated as the half difference between the 84 and the 16 percentile limits) of the local density profiles in the lower stratosphere is also larger up to 20 km with this most recent version. Only small changes (mainly a small increase of the median value above 30km) are observed for the  $NO_2$

vertical profiles in the validity altitude range 20 km-50 km. The median values of the  $NO_3$  profiles are larger with 6.0dh than with 6.0ab at altitudes higher than 30km (the  $NO_3$  validity altitude range is 25km-45km). The median of the aerosol extinction coefficient shows a significant increase (about 40% at the maximum in the Junge layer), as well as a decrease of the dispersion, especially at altitudes lower than 20km.

### 2.4. Comparison of $O_3$ profiles with external measurements

Examples of comparison of GOMOS  $O_3$  vertical profiles with ground-based and other satellite measurements made in close spatial and time coincidence are presented in Figure 2 to Figure 7.

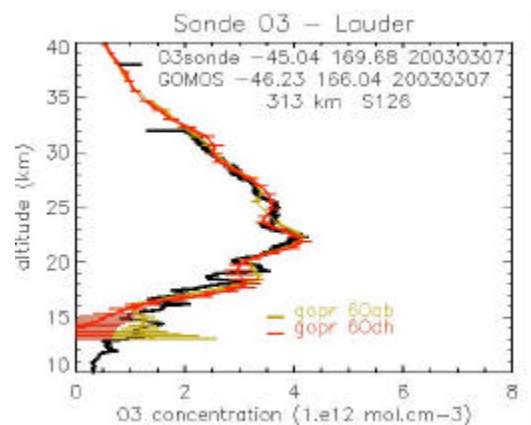


Figure 2: Vertical profile of  $O_3$  local density measured by ozonesounding at Lauder on 07/03/2003 and compared to GOMOS profile measured in close coincidence and retrieved with GOPR 6.0ab (green line) and with GOPR 6.0dh (red line). The location of the measurements (latitude, longitude), and the distance between the coincident measurements and the star ID are given in the plot label.

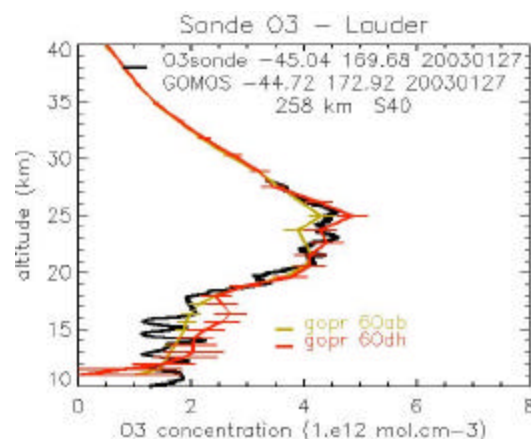


Figure 3: Same as Figure 2 for an ozonesounding at Lauder on 27/01/2003.

Those examples all show a general improvement of the comparison between the external measurement profile and the GOMOS

profile when the retrieval version used is 6.0dh instead of 6.0ab. For most comparisons shown, the main difference between the profiles by the two GOPR versions in the middle stratosphere is an increase of the O<sub>3</sub> local density. This yields a clear improvement of the comparison with the external profile at the O<sub>3</sub> maximum level. Figure 2 shows an example of comparison for which 6.0dh profile better describes vertical small-scale features also captured by the ozonesonde profile. However, in the lower stratosphere (comparisons with ozonesondes and satellite measurements), the O<sub>3</sub> local density for 6.0dh profile may show either larger or lower values than for 6.0ab profile, degrading or improving the comparison with the external measurement profile depending on cases.

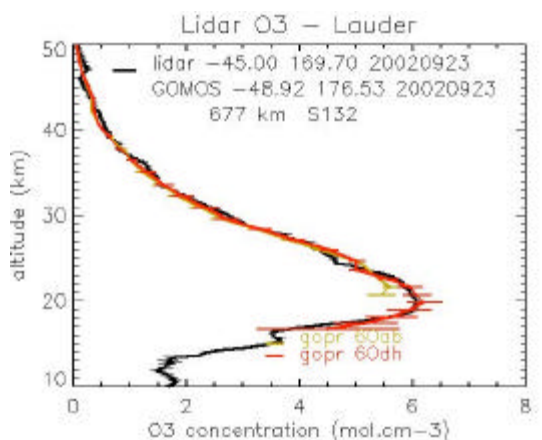


Figure 4: Same as Figure 2 for lidar measurement at Lauder on 23/09/2002.

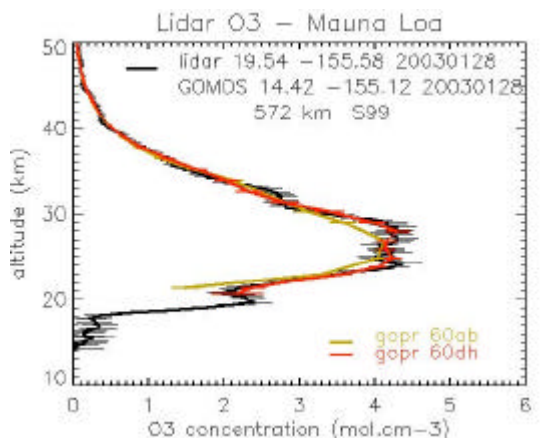


Figure 5: Same as Figure 2 for lidar measurement at Mauna Loa on 28/01/2003.

Other individual cases may illustrate a general degradation of the comparison between GOMOS and external profiles, when 6.0dh retrieval version is used instead of 6.0ab. A more global picture and a possible latitudinal dependence may be obtained by using larger datasets of individual coincidences and by performing statistical analysis of the discrepancy between the GOMOS profiles and the external measurements in coincidence [1].

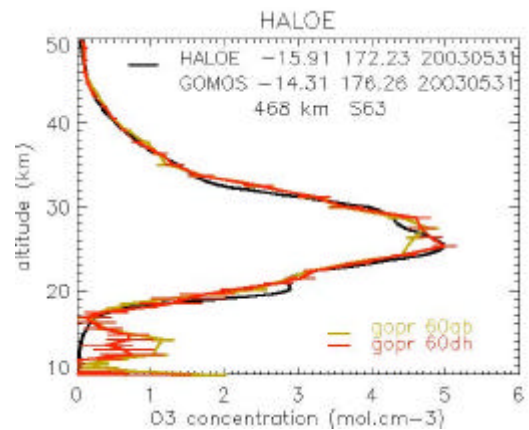


Figure 6: Same as Figure 2 for HALOE measurement on 31/05/2003.

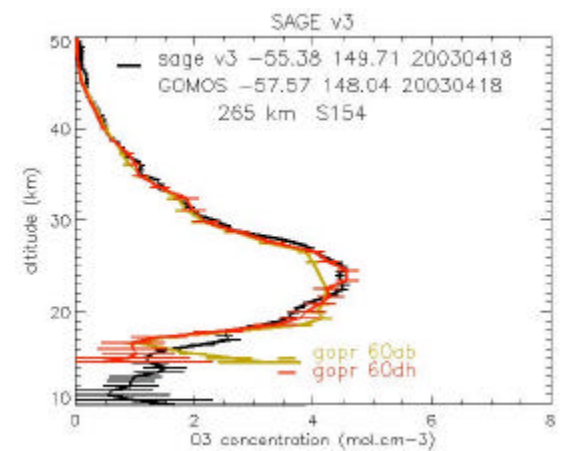


Figure 7: Same as Figure 2 for SAGE III measurement on 18/04/2003.

### 3. CONSISTENCY AND ROBUSTNESS OF THE RETRIEVAL ALGORITHM

The ENVISAT trajectory and the geometry of GOMOS measurements are such that the GOMOS swath from two successive orbits overlap significantly. By using those geometry specific features, it is possible to identify couples of GOMOS occultations measured with a time difference of one orbit (about 100 mn) and at nearby locations [2]. Because the measurements are made in close spatial and time coincidence, the impact of the natural variability on the possible differences between the vertical profiles is small. The comparison of the vertical profiles from coincident measurements made from the same star allows to check the consistency and the robustness of the algorithm. This is illustrated in Figure 8 and Figure 9 with the comparison of O<sub>3</sub> vertical profiles retrieved with 6.0dh from the occultation of star 30 on two successive orbits. Those occultations were measured in straylight illumination conditions. The agreement of the local density values and the error estimates for the two profiles in coincidence is excellent.

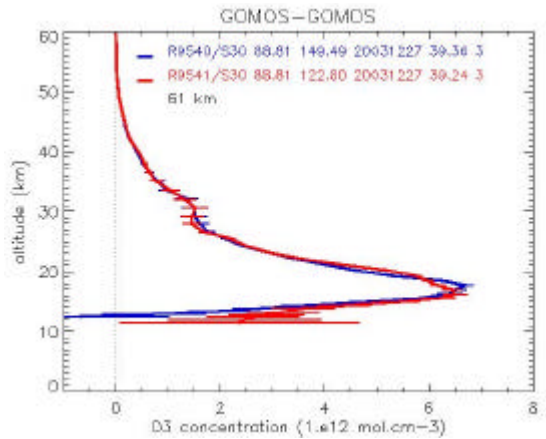


Figure 8: Vertical profiles up to 60km of  $O_3$  local density and error estimates retrieved with GPR 6.0dh from the occultation of star 30 measured on two successive orbits (R9540 : blue line and R9541: red line) in straylight illumination conditions. The distance between the profiles is 61km.

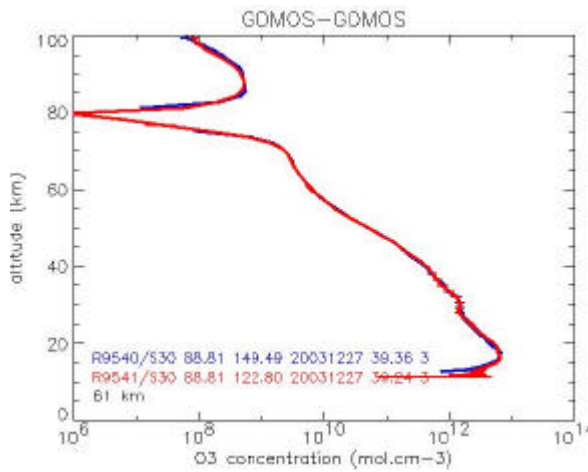


Figure 9: Same as Figure 8 up to 100 km (logarithmic scale).

#### 4. STAR CHARACTERISTICS AND SELECTION CRITERIA

The GOMOS-GOMOS coincidences may also be used to illustrate the impact of the star characteristics on the accuracy and on the quality of the vertical profiles. Due to this impact, it is recommended to apply selection criteria on the star effective temperature or on its visual magnitude in order to select the best quality vertical profiles [3, 4]. For  $O_3$  vertical profiles in the mesosphere, it is recommended to use only products from hot stars (see also [5]). For  $NO_2$  vertical profiles, it is recommended to use only products from bright stars (see also [6]).

##### 4.1. Vertical profiles of $O_3$ local density

We compare the  $O_3$  vertical profiles from the occultation of a hot star (S88) and from the occultation of a cool star (S14) (Figure 10). In the mesosphere, the profile from the cool star is much

noisier than the one from the hot star. The cool stars emit very little in the UV, and thus provide ozone retrievals in the mesosphere of lower quality than the hot stars [5]. For two stars of comparable effective temperature, no such discrepancy between the two profiles in the mesosphere is observed (Figure 11).

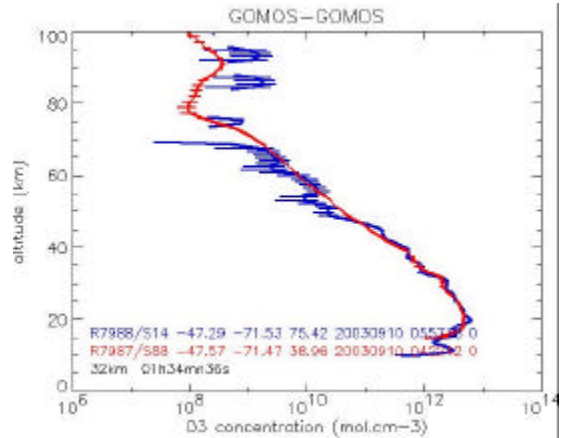


Figure 10: Vertical profiles of  $O_3$  local density and error estimates retrieved with GPR 6.0dh from two GOMOS-GOMOS coincidences (R7988/S14 : blue lines and R7987/S88: red lines). The distance between the profiles is 32 km.

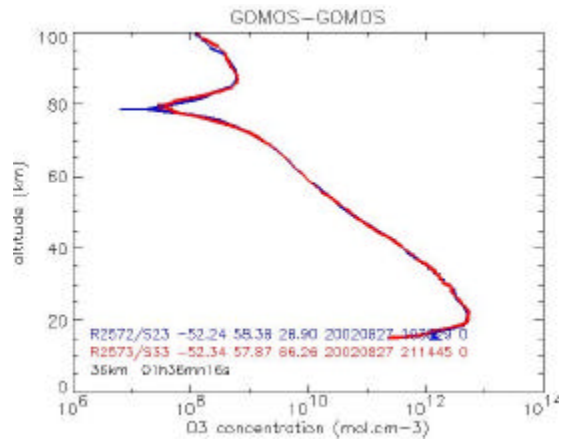


Figure 11: Same as Figure 10 for R2572/S23 (blue lines) and R2573/S33 (red lines). The distance between the profiles is 36 km.

##### 4.2. Vertical profiles of $NO_2$ local density

The comparison between  $NO_2$  vertical profiles from stars of different visual magnitude shows that the error bars are much larger for the profile from the dimmer star (Figure 12). At some altitude levels, the discrepancy between the local density of the two profiles is larger than the estimated contribution from a time difference of 100 mn (about 5%-10%).

Another example of coincidence for two bright stars (Figure 13) shows that the profiles are in good agreement; the error bars of both profiles are much smaller than for the dimmer star of the previous example.

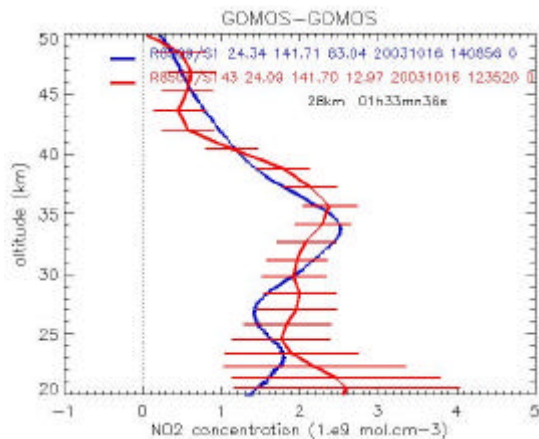


Figure 12: Vertical profiles of  $\text{NO}_2$  local density and error estimates retrieved with GOMOS 6.0dh from two GOMOS-GOMOS coincidences (R08509/S1: blue lines; R8508/S143: red lines). The distance between the profiles is 28 km.

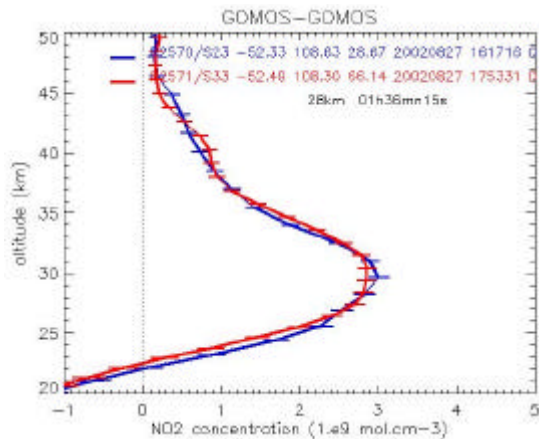


Figure 13: Same as Figure 12 for R2570/S23 (blue lines) and R2571/S33 (red lines). The distance between the profiles is 28 km.

## 5. Vertical profiles of $\text{O}_2$ local density

The local density values of  $\text{O}_2$  for a set of vertical profiles are compared to the  $\text{O}_2$  values inferred from ECMWF air density values.

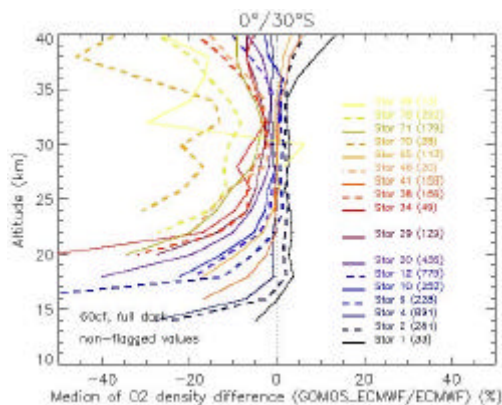


Figure 14: Vertical profiles of the median of the relative difference (%) between  $\text{O}_2$  local density values from GOMOS measurements and  $\text{O}_2$  values inferred from

ECMWF data. Results are plotted between 10km and 40km for measurements at low latitudes of the Southern hemisphere, and for several stars.

Results for several stars (ID between 1 and 99) and for measurements at low latitudes of the Southern hemisphere are presented in Figure 14 for altitudes between 10km and 40km. For the brightest stars (star ID between 1 and 12), the median difference ranges between -5% and +5%. For stars of lower brightness (star ID between 20 and 46), the median difference ranges between 0 and -10%. For dim stars (star ID between 70 and 99), the median difference ranges between -10% and large negative values, except for stars 41 and 65 showing small values of the median difference similar to the ones from the brightest stars.

## 6. REFERENCES

- [1] Y. Meijer et al., Pole-to-pole validation of GOMOS ozone profiles by the Envisat Quality Assessment with Lidar (EQUAL) project. *Proc. 3<sup>rd</sup> Workshop on the Atmospheric Chemistry Validation of Envisat (ACVE-3)* (Ed. D. Danesy), ESA SP-642, ESA Publications Division, Noordwijk, The Netherlands, 2006.
- [2] M. Guirlet et al., Comparison of GOMOS Level 2 products for measurements in close coincidence, *Proc. 3<sup>rd</sup> Workshop on the Atmospheric Chemistry Validation of Envisat (ACVE-3)* (Ed. D. Danesy), ESA SP-642, ESA Publications Division, Noordwijk, The Netherlands, 2006.
- [3] Disclaimer for GOMOS Level 1b and Level 2 products: <http://envisat.esa.int/dataproducts/availability/disclaimers/>
- [4] GOMOS Product Handbook, 2007: <http://envisat.esa.int/dataproducts/gomos/>
- [5] E. Kyrölä et al., Night-time ozone profiles in the stratosphere and mesosphere by GOMOS on ENVISAT, *J. Geophys. Res.*, Vol. 111, D24306, 10.1029/2006JD007193, 2006.
- [6] A. Hauchecorne et al., First simultaneous global measurements of nighttime stratospheric  $\text{NO}_2$  and  $\text{NO}_3$  observed by GOMOS/Envisat in 2003, *J. Geophys. Res.*, Vol. 110, D18301, 10.1029/2004JD005711, 2005.

## 7. ACKNOWLEDGEMENTS

**HALOE v19:** Dr. J.M. Russell III (PI, Hampton University, VA) and of Dr. E. E. Remsburg (PS, NASA Langley Research Center, Hampton, VA), <http://haloedata.larc.nasa.gov/home/index.php>  
**SAGE III v3:** NASA Langley Research Centre EOSDIS Distributed Active Archive Centre, <http://www-sage3.larc.nasa.gov/>  
**Ozonesondes:** PI G. Bodeker; **lidar:** PI: D. Swart (Lauder), S. McDermid (Mauna Loa); ENVISAT Ground-based Measurement and Campaign Database at NILU (<http://nadir.nilu.no/calval/>)

Table 1: Main configuration changes implemented in GOPR 6.0dh (Level 2) and compared to GOPR 6.0ab.

	6.0ab	6.0dh
<b>Aerosol law</b>	$1/\lambda$	$a + b\lambda + c\lambda^2$
<b>Cross-sections</b>	all species: GOMOS c.s.	O <sub>3</sub> : ORPHAL c.s.; others: GOMOS c.s.
<b>Air</b>	retrieved	not retrieved, fixed to ECMWF
<b>Error budget</b>	no additional turbulence error	additional turbulence error for O <sub>3</sub> , NO <sub>3</sub> and aerosols
<b>Flagging strategy</b>	Systematic flagging of negative density values	No systematic flagging of negative density values
<b>H RTP</b>		Improvement of the H RTP retrieval algorithm

Table 2: Visual magnitude and effective temperature of stars of which products are presented above.

Star ID	Visual magnitude	Effective T (K)	Star ID	Visual magnitude	Effective T (K)	Star ID	Visual magnitude	Effective T (K)
1	-1.44	11000	29	1.672	10200	65	2.204	4400
2	-0.736	7000	30	1.694	30000	70	2.246	39000
4	-0.01	5800	33	1.766	30000	71	2.246	7700
9	0.453	24000	34	1.793	23000	78	2.304	28000
10	0.610	28000	38	1.836	11000	88	2.448	20000
12	0.775	30000	40	1.859	7100	99	2.575	26000
14	0.87	3000	41	1.860	4100	126	2.770	4250
20	1.253	30000	46	1.954	10600	132	2.803	6900
23	1.502	26000	63	2.15	2800	154	2.899	5700

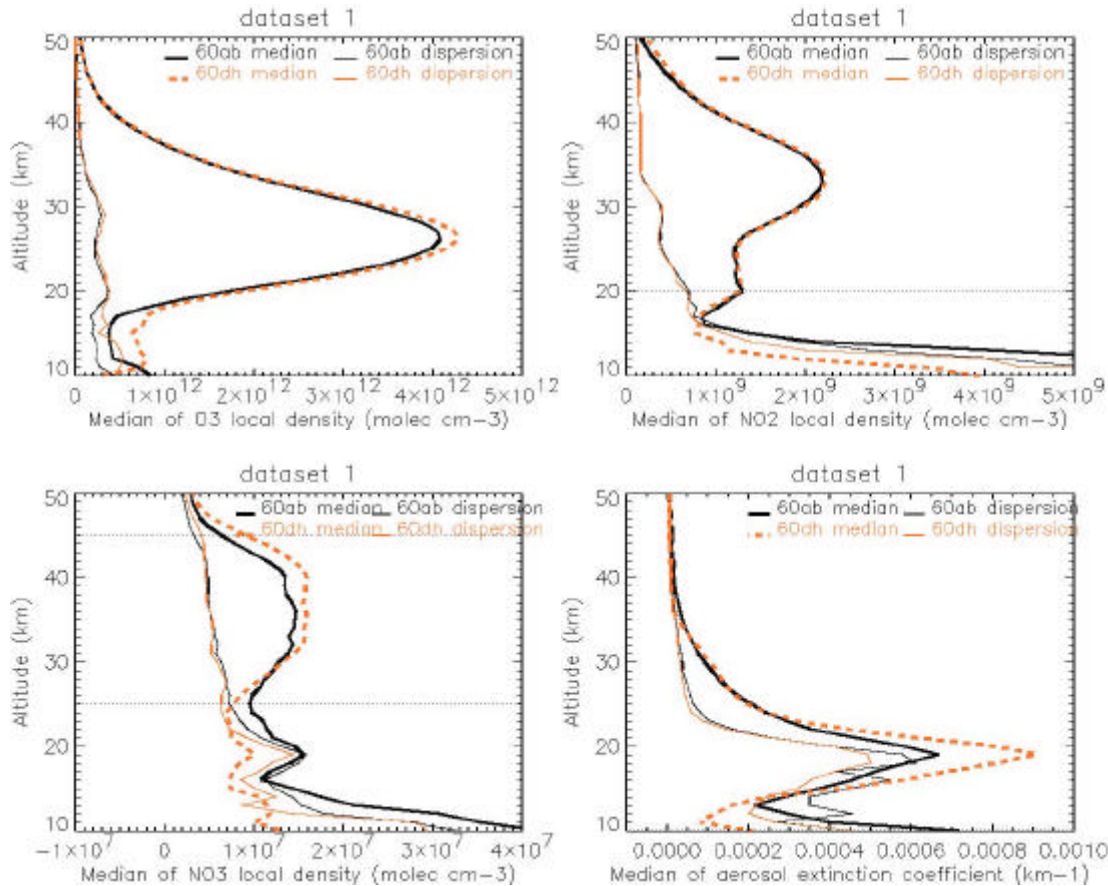


Figure 15: Median (thick lines) and dispersion (thin lines) of the vertical profiles of the local density of O<sub>3</sub> (top row, left figure), NO<sub>2</sub> (top row, right figure), NO<sub>3</sub> (bottom row, left figure) and of the aerosol extinction coefficient (bottom row, right figure). The dispersion is calculated as the half difference between the 84 and the 16 percentile limits. Results are plotted for a testing dataset of more than 500 occultations of star 29 measured at low latitudes between December 2002 and February 2003, and processed with GOPR version 6.0ab (black solid lines) and with GOPR version 6.0dh (orange lines). Horizontal lines on NO<sub>2</sub> and NO<sub>3</sub> plots indicate the limits of validity of the altitude range for those two species as stated in the disclaimer and in the Product Handbook.